

1 **Supramolecular biosolvents made up of self-assembled rhamnolipids: synthesis and**
2 **characterization**

3 **Encarnación Romera-García¹, Ana Ballesteros-Gómez^{1*}, Soledad Rubio¹**

4 ¹Department of Analytical Chemistry, University Institute of Nanochemistry, Faculty of
5 Science, University of Córdoba, Marie Curie Annex Building, Campus of Rabanales,
6 14071 Córdoba, Spain

7 *Corresponding author. Tel.: +34 957 218 644; fax: +34 957 218 644. E-mail address:
8 ana.ballesteros@uco.es.

9

10 **Abstract**

11 Simple coacervation of surfactants constitutes a powerful bottom-up strategy for the
12 production of tailored supramolecular solvents (SUPRASs), which feature outstanding
13 properties in extraction processes. In this study, we develop for the first time SUPRASs
14 made up from biosurfactants (produced by microorganisms) as a greener alternative to
15 synthetic surfactants. Rhamnolipids (RLs) were selected for this purpose due to their green
16 properties and their high potential for industrial applicability. BioSUPRASs were
17 spontaneously produced at room temperature from aqueous solutions of rhamnolipids
18 (RLs) by salt-induced coacervation (NaCl, Na₂SO₄ or NH₄CH₃CO₂). RLs quantitatively
19 incorporated into the bioSUPRAS phase, so that the process had high atom economy. The
20 boundaries for the coacervation region were delimited as a function of RL and salt
21 concentration and equations were derived to predict the volume of bioSUPRAS from the
22 composition of the synthesis mixture. The composition of bioSUPRASs could be tailored
23 by modifying the concentration of the coacervation-inducing salt. BioSUPRAS
24 aggregates were characterized by dynamic light scattering and cryo-scanning electron
25 microscopy and consisted of vesicles in a size range from nm to μm. These aggregates
26 offer a variety of interactions for solute solubilisation (dispersion, ionic, dipole-dipole
27 and hydrogen bonding), different polarity microenvironments (RL head group, RL
28 hydrocarbon chains, vesicle aqueous cavity) and a huge number of binding sites (RL
29 concentration varied from 205 to 444 g·L⁻¹). The potential of bioSUPRASs for efficient
30 extraction was illustrated by the recovery of highly polar ionic dyes from water with
31 yields above 94%. The compliance of RL-based bioSUPRASs with the twelve principles
32 of green chemistry is discussed.

33

34 **Keywords:** supramolecular solvent (SUPRAS), biosurfactant, rhamnolipid, salt-induced
35 coacervation, vesicles, extraction.

36

37 **1. Introduction**

38 The design and production of green solvents with properties that match specific chemical
39 objectives (extraction or purification processes, catalysis, etc.) constitute a strategic
40 priority within the framework of green chemistry.¹ The global market of green solvents,
41 valued at \$7 billion in 2018, is estimated to grow at an annual rate of 7.5% in the next
42 decade.² Key drivers for this demand are the stringent regulations on VOC emissions, the
43 toxicity of conventional solvents and the volatility of petrochemical prices.^{3,4}

44 Green solvents are commonly defined as those that do not exhibit health, safety, and
45 environmental concerns and that are characterized by a reduced life cycle impact.^{5,6} They
46 are expected to meet twelve criteria,⁷ although unfortunately, there is not any solvent that
47 fulfils all of them. Intensive research efforts over the two last decades have enabled the
48 synthesis of innovative green solvents (e.g. bio-based solvents, ionic liquids, deep
49 eutectic mixtures, supercritical fluids) and the development of breakthrough applications
50 in organic synthesis, catalysis, biotransformations and/or separations.⁸⁻¹⁰ However, there
51 is still a long way to go and many issues need to be satisfactorily resolved (solvent
52 performance, energy-saving synthesis processes, availability, etc.).⁷

53 Supramolecular solvents (SUPRASs)¹¹ constitute other suitable alternative to
54 conventional organic solvents for extraction processes. SUPRASs are nanostructured
55 liquids synthesized from the self-assembly and coacervation of amphiphiles through a
56 bottom-up approach (**Figure ESI1**).¹² SUPRAS synthesis involves, first, the spontaneous
57 *self-assembly* of amphiphiles into three-dimensional aggregates (e.g. micelles or vesicles)
58 above a critical aggregation concentration (*cac*) to generate a colloidal system (**Figure**
59 **ESI1**). Aggregation of amphiphiles at *cac* is considered a *start-stop* process,¹³⁻¹⁵ being
60 the *start* driven by the solvophobic effect¹⁶ and the *stop* arising from the repulsions among
61 amphiphile head groups.^{17,18} Secondly, *coacervation* (i.e. separation into two liquid
62 phases in colloidal systems)^{19,20} must be produced by the growth of the aggregates in the
63 colloid, and this involves reducing the repulsions among the amphiphilic head groups that
64 stopped aggregation at *cac*.¹⁷ How to achieve this aim mainly depends on amphiphile
65 structure. For ionic amphiphiles, coacervation is accomplished by adding an organic²¹ or
66 inorganic²² counterion or fixing the pH below the pKa of the ionic group.²³ The growth
67 of non-ionic aggregates is mainly driven by increasing the temperature²⁴ or by adding a
68 poor solvent for the amphiphile that is miscible with the solvation solvent.²⁵ In all cases,

69 oily coacervate droplets are spontaneously produced and form clusters that separate as a
70 new colloid-rich phase (coacervate phase or SUPRAS). The coacervate droplets keep as
71 individual entities and are in equilibrium with the bulk solution containing the amphiphile
72 at the *cac* (**Fig. ESI1**). The overall process can be considered an essentially energy-saving
73 synthesis, with 100% selectivity for SUPRAS formation and amphiphile conversions
74 above 90%²⁶ that can approach 100% by applying strategies to reduce the *cac*.²⁷

75 SUPRASs have long proved unique features for the simultaneous, efficient and fast
76 extraction of organic compounds in a wide polarity range,^{28,29} metal ions³⁰ and
77 proteins^{31,32} from both liquid and solid samples. The superior performance of SUPRASs
78 in extraction processes compared to molecular solvents mainly arise from three
79 characteristics.²⁹ First, the *different polarity microenvironments* present in SUPRAS
80 aggregates (e.g. polar at the head groups and nonpolar at the hydrophobic moieties),
81 which allows the simultaneous extraction of both polar and nonpolar compounds from
82 aqueous media. Secondly, *the multiple binding sites* owing to the huge concentration of
83 amphiphile in SUPRAS (0.1-1 mg· μL^{-1}). This characteristic, along with the mixed
84 mechanisms available for solute solubilization, allows efficient extractions at low
85 SUPRAS/sample ratios. Thirdly, the *large surface area* of SUPRASs arising from the
86 coacervate droplets that make them up, which enables fast solute mass transfer in
87 extraction processes.

88 These characteristics have been long exploited for the development of innovative sample
89 treatments in chemical analysis,^{11,28,29,33} and, more recently, for the extraction of
90 bioactives from vegetal biomass and agrifood residues^{34,35} and for wastewater
91 treatment.^{36,37} The reversible character of SUPRAS nanostructures, which are formed
92 through non-covalent interactions, constitutes an excellent opportunity for the production
93 of environment-responsive SUPRASs. This property has allowed the synthesis of
94 SUPRASs with restricted access properties that are able to exclude major matrix
95 interferences²⁵ and it has been exploited to produce carotenoid oleoresins at a much lower
96 cost than those produced with supercritical fluids.³⁸

97 SUPRAS meet some outstanding green criteria⁷ (e.g. use of energy-saving and high atom-
98 economy synthesis processes, exhibition of remarkable performances for some chemical
99 objectives, low volatility and flammability, etc.). However, surfactants used up to date
100 are petrochemical-based (a non-renewable resource) and only partially biodegradable
101 (sometimes producing toxic degradation products), e.g. alcohol and alkylphenyl

102 ethoxylates, alkanols, alkyl sulphate and sulphonate salts, gemini surfactants, alkyl
103 ammonium salts, etc.).¹¹ Furthermore, SUPRAS synthesis often requires the use of
104 organic co-solvents, such as methanol or tetrahydrofuran,²⁶ highly acidic conditions (3-5
105 M HCl)²³ or high temperature,²⁴ this compromising their sustainability and hindering
106 large-scale application. Some recent developments have been made by our research group
107 to produce low toxicity SUPRAS which were made up of (synthetic) alkyl-carboxylic
108 acids and fatty alcohols in mixtures of ethanol and water.^{35,39,40} However, the use of
109 organic solvent and surfactants from not renewable sources compromised their green
110 properties.

111 In this study, we propose for the first time the production of supramolecular biosolvents
112 (bioSUPRASs) by coacervation of biosurfactants with green agents. The developed
113 bioSUPRASs are expected to better meet the criteria set for green solvents.⁷
114 Biosurfactants are amphiphilic compounds mainly produced by bacteria, yeasts and
115 fungi.⁴¹ They have interesting properties to be used as SUPRAS ingredients, including
116 low toxicity, biodegradability, high stability in a wide range of pH, temperature and
117 salinity, low *cac*, production from renewable resources and scale-up capacity.⁴²

118 Rhamnolipids (RLs) are produced by bacteria of the genus *Pseudomonas* or *Burkholderia*
119 and consist of one or two L-rhamnose (Rha) residues linked to one or two 3-hydroxyfatty
120 acids of various chain lengths, typically ranging from eight to sixteen.^{43,44} Among
121 biosurfactants from microbiological sources, e.g. glycolipids (rhamnolipids,
122 sophorolipids, trehalose lipids and mannosylerythritol lipids) and lipopeptides (surfactin
123 and lichenysin), RLs have been recognized as the best alternatives to synthetic surfactants
124 with a market value of \$2.8 billion in 2023.⁴⁵ They stand out because of their eco-friendly
125 properties and use in a broad range of products and applications, such as food,
126 pharmaceutical, cosmetics, detergents and cleaning agents, bioremediation, enhanced oil
127 recovery and agriculture.^{46,47}

128 RLs self-assemble into micelles and vesicles in aqueous solutions,⁴⁸⁻⁵⁰ so they produce
129 colloidal systems above the *cac* and, in principle, they have the potential to undergo
130 coacervation. The liquid-liquid phase separation of biosurfactants in colloidal systems
131 remains virtually unexplored, and to the best of our knowledge, only the coacervation of
132 the glycolipid mannosyl-erythritol lipid-A in water has been reported so far.⁵¹ In this
133 paper, the production of bioSUPRASs from RLs under the action of several salts (NaCl,
134 Na₂SO₄ and NH₄CH₃CO₂) was investigated. Coacervation regions for the different

135 bioSUPRASs were delimited and prediction equations for the generated volume under
136 different synthesis conditions were proposed. The chemical composition and
137 physicochemical properties of bioSUPRASs were determined and their nanostructures
138 were characterized. Extraction properties of bioSUPRASs were evaluated using anionic
139 and cationic dyes as model compounds.

140

141 **2. Material and methods**

142 **2.1 Chemicals**

143 All chemicals were used as supplied. The rhamnolipid (RL) employed for bioSUPRAS
144 synthesis (CAS number: 869062-42-0, 90% purity) was purchased from Sigma-Aldrich
145 (Madrid, Spain). According to product specifications, it contains a mixture of decanoic
146 acid, 3-(((6-deoxy-2-O-(6-deoxy- α -L-mannopyranosyl)- α -Lmannopyranosyl)oxy)-, 1-
147 (carboxy methyl)octyl ester (Rha-Rha-C₁₀-C₁₀) and 1-(carboxymethyl)octyl 3-(((6-
148 deoxy- α -L-mannopyranosyl)oxy)decanoate (Rha-C₁₀-C₁₀), **Figure ESI2**. Type II water
149 was obtained from an Elix® Essential 3 water purification system (Merck Millipore,
150 Madrid, Spain). Sodium chloride (NaCl, ACS reagent, $\geq 99.0\%$ purity), sodium sulphate
151 anhydrous (Na₂SO₄, tested according to Ph. Eur., 99.5% purity) and ammonium acetate
152 (NH₄CH₃CO₂, $\geq 98.0\%$ purity) were supplied by Sigma-Aldrich (Madrid, Spain).
153 Methanol (CH₃OH, gradient grade for HPLC, Reag. Ph. Eur., $\geq 99.8\%$ purity) was
154 purchased from VWR (Barcelona, Spain). Trypan blue (C₃₄H₂₄N₆O₁₄S₄Na₄) was obtained
155 from Fluka (Madrid, Spain) and malachite green oxalate salt
156 (C₂₃H₂₅N₂·C₂HO₄·0.5C₂H₂O₄, certified by BSC, $\geq 90\%$ purity) was supplied by Sigma-
157 Aldrich (Madrid, Spain).

158

159 **2.2 Apparatus**

160 BioSUPRAS synthesis required a vortex mixer and a centrifuge. The following devices
161 were used for the synthesis of the whole range of bioSUPRASs: a Reax Top vortex mixer
162 equipped with an attachment for centrifuge microtubes from Heidolph (Schwabach,
163 Germany), a Vortexer vortex mixer equipped with an attachment for different size tubes
164 from Heathrow Scientific (Vernon Hills, IL, USA), a MPW-350R high speed brushless
165 centrifuge equipped with an angle rotor 36×2.2/1.5 mL from MPW Med. Instruments

166 (Warsaw, Poland) and a Mixtasel BLT digitally regulated centrifuge equipped with an
167 angle rotor 16×15 mL from JP Selecta (Barcelona, Spain). A 831 KF Coulometer with
168 generator electrode without diaphragm from Metrohm (Herisau, Switzerland) and a
169 EA3000 elemental analyzer from EuroVector Srl (Milan, Italy) were respectively used
170 for the determination of water and rhamnolipid contents in the bioSUPRASs. A 848
171 Titrino plus from Metrohm (Herisau, Switzerland) and a LP 2000 Turbidity Meter from
172 Hanna Instruments (Guipúzcoa, Spain) were respectively employed for the quantification
173 of Cl^- and SO_4^{2-} in the equilibrium solution. The electron micrographs were acquired with
174 an EVO LS 15 scanning electron microscope from Zeiss (Oberkochen, Germany) and the
175 size of the RL aggregates was measured using a Zetasizer NANO ZSP from Malvern
176 Panalytical (Madrid, Spain). An UV-Vis spectrophotometer (model 99-90287) from
177 BioTek Instruments (Winooski, VT, USA) was used for quantifying remaining dyes in
178 water samples after extraction with bioSUPRASs.

179

180 **2.3 Phase diagrams for ternary mixtures of rhamnolipid/water/salt**

181 Phase diagrams were constructed in order to define the rhamnolipid/water/salt ratios
182 required for bioSUPRAS production. For this purpose, the biosurfactant was dissolved in
183 water into 15 mL centrifuge tubes and, then, the salt was added in order to promote
184 coacervation. The mixture was vortex-shaken for 5 min to favour the contact between
185 their components and then centrifuged (3,500 rpm, 30 min) to accelerate phase separation.
186 Rhamnolipid and salt (NaCl , Na_2SO_4 and $\text{NH}_4\text{CH}_3\text{CO}_2$) concentrations were varied in the
187 intervals of 0.09-9% (w/v) and 0-3 M, respectively. All experiments were performed in
188 duplicate and the temperature was kept constant at 25 °C. Boundaries of phase diagrams
189 were defined through visual observation. The formation of two immiscible liquid phases
190 was the criterion used to determine the formation of bioSUPRASs, otherwise
191 homogeneous liquid phases or liquid-solid phases were observed.

192

193 **2.4 BioSUPRAS volume and density**

194 The volume of solvent that was formed within the coacervation region was measured for
195 bioSUPRASs induced by NaCl and Na_2SO_4 . It was calculated by measuring its height in
196 the cylindrical tube with a digital calliper. The statistics package Statgraphics Centurion
197 XVI.II was used to fit a model, through non-linear regression, that could predict the

198 volume of bioSUPRAS as function of the composition of the ternary mixture. The density
199 of bioSUPRASs synthesized under different conditions was calculated by weighting a
200 given volume of coacervate in an analytical balance. The experiments were conducted in
201 duplicate.

202

203 **2.5 Chemical composition of bioSUPRASs**

204 The concentration of water, rhamnolipid and salt in the bioSUPRASs (% , w/w) was
205 determined as function of the concentration of rhamnolipid and salt in the synthesis
206 mixture. Coulometric Karl Fischer titration was used to determine the water content. For
207 that, an aliquot of bioSUPRAS (50 μ L) was weighted and dissolved in methanol up to 2
208 mL in a centrifuge microtube. After it was vortex-shaken (2 min) and centrifuged (15,000
209 rpm, 5 min), 100 μ L of the supernatant was injected into the titration cell. All experiments
210 were made in duplicate.

211 The concentration of rhamnolipid in the bioSUPRASs (and in the equilibrium solutions)
212 was estimated from the carbon content through elemental microanalysis. For this purpose,
213 an aliquot of 1-5 mg of bioSUPRAS was weighted in a tin capsule and then sealed and
214 placed into the autosampler. The sample was combusted in a reactor at 1020 $^{\circ}$ C for 4.4
215 sec, in a temporarily enriched oxygen atmosphere (7 mL, Δ PO₂=25 kPa). The combustion
216 products were carried by a helium stream (110 kPa) through an oxidation catalyst and a
217 copper reducer. Finally, the gases were separated in a stainless steel packed GC column
218 at 90 $^{\circ}$ C and detected using a thermal conductivity detector. The run time was 120 sec.

219 The concentration of NaCl and Na₂SO₄ incorporated into the bioSUPRAS were
220 calculated as the difference among the initial salt concentration added to the synthesis
221 mix and the concentration measured in the equilibrium solution after the coacervation
222 process. Cl⁻ was determined by the classic precipitation titration with AgNO₃ (0.1 M) in
223 acid medium which was monitored by potentiometric measurement with a silver sensor
224 (method AOAC 963.05). SO₄²⁻ was measured by the classic turbidimetric method based
225 on addition of BaCl₂ and a stabilizing solution to measure the barium sulfate turbidity
226 (method EPA 9038).

227

228

229 **2.6 Characterization of the bioSUPRAS structure**

230 The hydrodynamic diameter of RL aggregates in bioSUPRASs produced from different
231 salt concentrations was measured by dynamic light scattering (DLS). The measurements
232 were carried out in 12 mm square polystyrene cuvettes placed in a thermostatic holder
233 (25 °C), and data were collected at 173° scattering angle. The intensity-based size
234 distribution was calculated through non-negative least squares (NNLS) analysis. Each
235 bioSUPRAS was prepared in duplicate and each sample was analysed three times.

236 The morphology of the aggregates was visualized through cryo-scanning electron
237 microscopy (cryo-SEM). The preparation of the samples started by pouring a drop of
238 bioSUPRAS between two rivets and plunging it in liquid nitrogen. Then, the sample was
239 inserted into the cryogenic ante-chamber (-120 °C, $3.2 \cdot 10^{-6}$ mbar), where it was fractured
240 to expose a cross section of the drop. The superficial ice was removed by sublimation and
241 the aggregates were then revealed. For this purpose, the temperature varied (5 °C/min) up
242 to -90 °C, where it kept constant for 15 minutes, and then, once again lowered to -120 °C.
243 Finally, the sample was transferred to the microscope where the electron micrographs
244 were acquired at -120 °C.

245

246 **2.7 BioSUPRASs-based extraction of dyes**

247 The extraction capacity of bioSUPRASs was investigated by extracting two dyes (trypan
248 blue and malachite green) from water. For this purpose, different bioSUPRASs (0.9 and
249 4.5% of RL (w/v), 1 and 1.5 M of NaCl) were synthesized directly in tap water samples
250 (4 mL) containing the dyes at $7 \text{ mg} \cdot \text{L}^{-1}$. The mixture was vortex-shaken (10 min) to favour
251 the extraction and centrifuged (3,500 rpm, 30 min) to accelerate the separation of the
252 bioSUPRAS. The remaining concentrations of trypan blue and malachite green in the
253 equilibrium solution were monitored at 607 and 617 nm, respectively. All experiments
254 were conducted in duplicate. Calibration was carried out by preparing aqueous solutions
255 containing the dyes in the concentration range of $0.2\text{-}10 \text{ mg} \cdot \text{L}^{-1}$.

256

257 **3. Results and discussion**

258 **3.1 Salt-induced synthesis of bioSUPRASs from rhamnolipids**

259 RLs are produced, mostly by *Pseudomonas Aeruginosa*, as a mixture of mono-Rha and
260 di-Rha homologues whose composition depends on the bacterial strains, substrates and
261 culture conditions.⁴⁶ The fermentation broth contains RL homologues and a mixture of
262 unfermented substrates, polysaccharides, salts, amino acids, proteins and other metabolic
263 products.⁴³ Purification of RLs can contribute up to 50-80% of the total production cost.⁴⁴
264 The commercially available RL used in this study (90% purity) consisted of a mixture of
265 anionic Rha-C₁₀-C₁₀ and Rha-Rha-C₁₀-C₁₀ (**Figure ESI2**) and it was obtained using the
266 fermentation of canola oil and/or vegetable oil by *Pseudomonas Aeruginosa*. It has been
267 long proved that both single and mixed Rha-C₁₀-C₁₀ and Rha-Rha-C₁₀-C₁₀, with purities
268 in the range of 60-100%, are able to give colloidal systems, so they were considered
269 excellent candidates for producing bioSUPRASs.^{48,49,52-54} Given that the RL cost greatly
270 increases with the level of product purity, and that common RL impurities are not
271 amphiphilic and consequently are not expected to give coacervates, we decided to
272 investigate the production of bioSUPRASs using a non-highly purity RL product (90%
273 purity).

274 **Table ESI1** shows the reported critical aggregation concentration (*cac*) of colloidal
275 systems produced from Rha-C₁₀-C₁₀ and Rha-Rha-C₁₀-C₁₀ at different pH values,
276 electrolyte concentration and product purity.^{48,49,52-54} The reported *cac* for RLs (pK_a 5.6-
277 5.9 for the carboxylic groups present in these biosurfactants) is higher for the anionic
278 form compared to the non-ionic one, owing to the greater repulsion between anionic RL
279 molecules (e.g. *cac* values were 1.6-50 times higher at pH 7.4 or 9 than at pH 4 or in ultra-
280 high quality water, **Table ESI1**).⁴⁹ On the other hand, electrolytes such as NaCl had a
281 negligible or limited effect on the *cac* of non-ionic RLs but they considerably reduced the
282 *cac* of anionic RLs.^{48,52-54} This reduction is the consequence of the shielding of the
283 negative charge and dehydration of carboxylate groups by Na⁺ ions, which results in the
284 formation of a close-packed aggregate.⁴⁸ *Cac* values changed similarly against pH and
285 with the presence and concentration of electrolytes independently of the type of RL
286 homologue and product purity (**Table ESI1**).

287 Taking into account the aggregation behaviour in colloidal systems of RLs, the formation
288 of bioSUPRASs was tried from colloidal dispersions of anionic RLs in the presence of
289 electrolytes. Three salts were investigated for this purpose, namely sodium chloride,
290 sodium sulphate and ammonium acetate. **Figure 1** shows the phase diagrams obtained at
291 25 °C from the three different rhamnolipid/water/salt ternary mixtures. They were plotted

292 as the concentration of salt (M) versus the percentage of RL (w/v) in the colloidal system.
293 The study was restricted to biosurfactant concentrations in the range of 0.09-9% (w/v)
294 because, as it will be commented later, the most interesting applications of SUPRASs in
295 extraction processes involve a low concentration of this ingredient.

296 Three regions were always observed in the phase diagrams as the concentration of salt
297 increased; an isotropic solution, two immiscible liquid phases (i.e. the region for
298 bioSUPRAS formation) and a liquid-solid phase region where the biosurfactant
299 precipitated. Thus, the three salts were able to induce the coacervation of RLs, although
300 both the minimum concentration required for liquid phase separation, that is an indicator
301 of their coacervation strength, and the extension of the coacervation region, depended on
302 the nature of the salt. The ordering of salts in terms of coacervation strength was
303 $\text{NH}_4\text{CH}_3\text{CO}_2 > \text{Na}_2\text{SO}_4 > \text{NaCl}$. The formed bioSUPRASs separated from the equilibrium
304 solution as an upper (Na_2SO_4 -induced) or bottom ($\text{NH}_4\text{CH}_3\text{CO}_2$ - and NaCl -induced)
305 phase.

306 Although the microscopic origins of coacervation still remain elusive and there are only
307 few precedents of electrolyte-inducing coacervation of ionic amphiphiles,^{55,56} it is widely
308 accepted that addition of salt to ionic colloidal systems causes destruction of the hydration
309 layer of surfactant head groups and decreases electrostatic repulsions.¹⁷ In this way, the
310 effective area per molecule at the interface diminishes and surfactant monomers can be
311 packed closer together leading to aggregate growth and liquid phase separation.⁵⁷ Each
312 salt is expected to have a specific influence on the coacervation of the ionic amphiphile,
313 whether it tends to adsorb in the interface between the amphiphile aggregate and water or
314 remains strongly hydrated in the bulk.⁵⁷ In addition, the effects of salts are concentration-
315 dependent; electrostatic interactions dominate at concentrations below 0.1 M and
316 dehydration is prevailing at intermediate concentration (0.1-2 M). At the highest
317 concentrations, most of the water is captured at the ion hydration spheres and salting-out
318 usually occurs.⁵⁸

319 Regarding the coacervation of RLs, the binding of RL carboxylate groups to Na^+ and
320 NH_4^+ will diminish electrostatic repulsions. Counterion binding to surfactant head groups
321 has been recently rationalised by the *law of matching water affinities* (LMWA), which
322 asserts that ion specificity to form contact ion pairs is favoured when their water affinities
323 match, this meaning that they share similar water hydration enthalpies ($\Delta H_{\text{hydration}}$).⁵⁹ As
324 a consequence, kosmotropic (highly hydrated) ions tend to pair together and chaotropic

325 (poorly hydrated) ions tend to form tight ion pairs. The sign of the Jones-Dole viscosity
326 coefficient (B) is a measure of ion hydration (positive for kosmotropic and negative for
327 chaotropic).⁵⁹ Carboxylate head groups are strongly hydrated (hydration number from 5
328 to 7)⁶⁰ and they are considered to be kosmotropic. So, they are expected to bind more
329 strongly to Na⁺ (kosmotropic, B: 0.086) than to NH₄⁺ (chaotropic, B: -0.007).⁵⁷

330 Considering that the coacervation strength of salts was in disagreement with the binding
331 strength of cations to RL carboxylate groups, the dehydration of head groups could be the
332 dominant mechanism for RL coacervation. RL headgroups count with big polar non-ionic
333 rhamnosyl groups (**Figure ESI2**). These groups are expected to be strongly hydrated and,
334 consequently, they could also be dehydrated by salt anions. In this respect, the water
335 *withdrawing power* of anions follows the sequence CH₃COO⁻ (kosmotropic, B: 0.250) >
336 SO₄⁼ (kosmotropic, B: 0.208 > Cl⁻ (chaotropic, B:-0.007). This trend was in agreement
337 with the coacervation strength of the salts (NH₄CH₃CO₂ > Na₂SO₄ > NaCl). Furthermore,
338 salting-out effects in the bulk solution can help to coacervation. This study shows that the
339 selection of both cations and anions are of primary importance for the coacervation of
340 ionic amphiphiles.

341 The formation region of the ammonium acetate-induced bioSUPRAS was very small
342 (**Figure 1**), which could hinder its production from low purity RLs. It was only formed
343 from RL percentages above 2.7%, which hampers its applicability in extraction processes
344 where high concentration factors are required. Consequently, we did not further
345 investigate this system. Both NaCl and Na₂SO₄, were selected as coacervation-inducing
346 agents for further study. They are nontoxic and have low cost and reactivity and high
347 stability, which makes them suitable for the scale-up of bioSUPRAS production.

348

349 **3.2 BioSUPRAS volume and density**

350 The volume of bioSUPRAS that was produced in the colloidal system (expressed as μL
351 of bioSUPRAS per mL of synthesis mixture) was a function of both the concentration of
352 rhamnolipid and of salt. This volume linearly increased with the concentration of
353 biosurfactant (**Figure 2 A, B**). The slopes and correlation coefficients of the linear
354 regression lines as a function of biosurfactant and at different concentrations of NaCl and
355 Na₂SO₄, are shown in **Table ESI2**. This linear dependence is common in SUPRAS

356 production since SUPRAS composition usually keeps constant as the experimental
357 conditions leading to coacervation (e.g. salt concentration) remain unchanged.¹¹

358 Regarding the effect of salts, results in **Figure 2 C, D** and **Table ESI2** clearly show that
359 the volume of bioSUPRAS decreased as the concentration of NaCl and Na₂SO₄ increased.
360 This behaviour suggests that bioSUPRAS composition is dependent on the concentration
361 of the coacervation-inducing agent and consequently, they are environment responsive.
362 **Figure ESI3** illustrates how the slopes of the linear regression lines decreased in the
363 presence of NaCl and Na₂SO₄. Slopes were lower for Na₂SO₄ than for NaCl, so we
364 measured smaller increments of bioSUPRAS volumes for Na₂SO₄ as the concentration of
365 biosurfactant increased. In general, as illustrated in **Figure ESI4**, a lower volume of
366 bioSUPRAS will be produced under the action of NaCl, except at the highest tested
367 concentrations of biosurfactant.

368 Non-linear regression was used to fit a model ($n_{NaCl}=55$, $n_{Na_2SO_4}=47$) which predicts the
369 volume of solvent produced as a function of the composition of the colloidal system:

$$370 \quad V_{\text{bioSUPRAS}} = \frac{\text{Rhamnolipid}}{(0.0200 \pm 0.0007) \cdot NaCl - (0.010 \pm 0.001)} - \frac{(292 \pm 21)}{NaCl} + (117 \pm 13) \quad [1]$$

$$371 \quad V_{\text{bioSUPRAS}} = \frac{\text{Rhamnolipid}}{(0.0319 \pm 0.0006) \cdot Na_2SO_4 - (0.0123 \pm 0.0007)} - \frac{(94 \pm 6)}{Na_2SO_4} + (112 \pm 4) \quad [2]$$

372 The dependent variable, $V_{\text{bioSUPRAS}}$, is the volume of bioSUPRAS ($\mu\text{L} \cdot \text{mL}^{-1}$), and the
373 independent variables, *rhamnolipid* and *NaCl/Na₂SO₄*, are the initial concentrations of
374 biosurfactant (% w/v) and salt (M) in the colloidal system. Equation 1 is valid within the
375 range: 2.7-9.0% (w/v) RL and 1.25-2.25 M NaCl; while equation 2 has the following
376 boundaries: 1.8-9.0% (w/v) RL and 1-1.75 M Na₂SO₄. The good capability of prediction
377 of these models was proved by their determination coefficients: $R^2_{\text{equation1}}=0.9951$,
378 $R^2_{\text{equation2}}=0.9991$ (**Figure ESI5**). These equations are of interest for application of
379 bioSUPRASs in extraction processes. Thus, for the extraction of contaminants,
380 bioactives, metabolites etc. from liquid samples, where the bioSUPRAS is generated in
381 the sample, the most favorable fractional bioSUPRAS phase volume (i.e. bioSUPRAS
382 volume/sample volume) will be obtained at the lowest and highest concentrations of RL
383 and salt, respectively, within the coacervation region. The fractional bioSUPRAS phase
384 volume could reach values down to ~0.03 (concentration factor of ~30) by using NaCl.
385 On the other hand, these equations also predict that for a given bioSUPRAS composition,
386 the highest solvent volumes will be produced at the highest concentrations of RL within

387 the coacervation region. This is interesting for the extraction of organic compounds from
388 solid samples, where the bioSUPRAS is previously generated in an aqueous medium, and
389 then separated from the equilibrium solution and stored until use. It was checked that
390 bioSUPRASs, once separated from the equilibrium solution, were stable at room
391 temperature in closed bottles for at least one month.

392 **Tables ESI3 and ESI4** show representative values for the density of the bioSUPRASs
393 produced from different percentages of RL and varying concentrations of NaCl and
394 Na₂SO₄, respectively. No significant differences in density were observed for each type
395 of bioSUPRAS under the different synthesis conditions. The mean values were 1.08±0.02
396 g·mL⁻¹ and 1.11±0.04 g·mL⁻¹ for bioSUPRASs formed with NaCl and Na₂SO₄,
397 respectively. The density values found in the literature for aqueous solutions of NaCl (1-
398 2.25 M, 20 °C) and Na₂SO₄ (1-1.75 M, 20°C) varied in the ranges of 1.04-1.08 and 1.13-
399 1.21 g·mL⁻¹, respectively. So, the bioSUPRAS formed as an upper (Na₂SO₄) or bottom
400 (NaCl) phase from the colloidal system depended on the salt used for its formation.
401 Depending on the particular application it may be operationally more advantageous that
402 the solvent remains either in the lower or upper part of the container.

403

404 **3.3 Chemical composition of bioSUPRASs**

405 **Table 1** shows representative results about the bioSUPRAS composition within the whole
406 region of coacervation. These results indicate that bioSUPRASs were primarily made of
407 RL and salty water, and that their composition was independent of RL concentration in
408 the synthesis mixture but significantly depended on salt concentration. Thus, as the
409 concentration of salt in the synthesis mixture raised, the water content in the bioSUPRASs
410 progressively decreased while the solvent gradually became more and more concentrated
411 with amphiphile. The reduction in water content fitted a negative linear relationship with
412 both NaCl and Na₂SO₄ (**Figure ESI6**).

413 These results confirm that both types of bioSUPRASs are environment responsive and
414 that their composition can be tuned according to the concentration of salt added to the
415 colloidal system. On the other hand, the same range of bioSUPRAS composition (i.e. RL:
416 19-40%, w/w and salty water: 81-62%, w/w, **Table 1**) can be obtained from both NaCl
417 and Na₂SO₄. However, the concentration of salt required to obtain a specific bioSUPRAS
418 will be dependent on the type of electrolyte. The percentage of RL in the bioSUPRASs

419 was in the same order of magnitude than that reported in bibliography for the synthetic
420 surfactant 9-methyl dodecanoate (20-33%, w/v), which coacervates from 0.86% (w/v) of
421 amphiphile and 1 M of salt (NaCl, KCl, NaSCN, KSCN) at 70 °C.⁶¹

422 RL residues were not detected in the equilibrium solutions above the quantitation limit of
423 the employed technique (~0.1% C, equivalent to ~3 mM rhamnolipid). As it has been
424 widely reported in coacervation-induced liquid phase separation processes,^{11,61} the
425 concentration of amphiphile in the equilibrium solution is expected to be near the critical
426 aggregation concentration (e.g. 0.03-0.05 mM in presence of 0.5-1 M NaCl for Rha-C10-
427 C10, see **Table ESI1**). Thus, the incorporation of RL to the bioSUPRAS was around
428 100% under all the experimental conditions and, consequently, the synthesis of RL by
429 coacervation at room temperature can be considered a high atom-economy process, in
430 addition to be energy-saving.

431 Finally, the water fraction in the bioSUPRAS kept the same salt concentration (± 0.05 M)
432 as that initially employed for the formation of the bioSUPRAS (~0.5-2.25 M in water),
433 which support the key role of the salt in the coacervation process.

434

435 **3.4 Characterization of bioSUPRAS structure**

436 The morphology and size of the RL aggregates in colloidal systems at different pHs and
437 concentrations of biosurfactant and salt have been widely investigated by electron
438 microscopy and DLS. **Table ESI5** shows representative results for anionic RLs in the
439 presence and absence of NaCl.^{48,52,54,62} In general, RL aggregates within several size
440 ranges (i.e. bimodal or multimodal distribution) co-exist in colloidal systems and become
441 bigger with increasing RL and salt concentration. Reported RL morphologies include a
442 broad variety of aggregates (e.g. micelles, vesicles, cubic lamellar phases, hexagonal
443 phases, etc.). Studies with RL concentrations as high as those found in bioSUPRASs (e.g.
444 205-444 g·L⁻¹) have not been undertaken so far (e.g. RL concentrations in **Table ESI5**
445 are within the range 0.07-3.6 g·L⁻¹).

446 The hydrodynamic diameters of the RL aggregates in bioSUPRASs were calculated by
447 DLS. **Figure 3** shows, as an example, the well-separated multimodal distribution obtained
448 for bioSUPRASs generated by NaCl. We observed aggregates within three size ranges of
449 5-14 nm, 42-400 nm and 500-4500 nm that shifted towards bigger sizes at NaCl
450 concentrations higher than 1.5 M (e.g. 23-170/200 nm, 300-1500/2000 nm; 2500/3000-

451 6500 nm). Results were in agreement with studies on RL aggregates in colloidal systems,
452 ^{48,52,54,62} which reported the coexistence of different self-assembled structures and bigger
453 sizes at increasing salt concentrations.

454 The morphology of bioSUPRAS aggregates was investigated with cryo-SEM. The
455 sample was fractured and the surface water was removed by controlled sublimation.
456 **Figures 4** and **5** show representative images for bioSUPRASs formed with Na₂SO₄ and
457 NaCl, respectively. They clearly show the formation of relatively big spherical structures
458 and internal cavities can be observed, thus confirming the formation of vesicles. The size
459 of the structures (from nm to μm) was in accordance with the results predicted by DLS
460 measurements. Micelles could be also present at the lowest size ranges observed by DLS
461 (e.g. 5-14 nm in **Figure 3 A**).

462 The same type of structures were observed for bioSUPRASs promoted by NH₄CH₃CO₂
463 as investigated by optical microscopy (**Figure ESI7**). This indicates that vesicles seems
464 to be the most energetically favourable structures in bioSUPRASs made up of RLs.

465

466 **3.5 Potential of bioSUPRASs for extraction processes**

467 BioSUPRASs made up of RL vesicles meet the characteristics to be excellent extractants
468 of organic compounds in a wide polarity range from both liquid and solid samples. They
469 provide microenvironments of different polarity (RL polar groups (-OH, -COO⁻), RL
470 hydrocarbon chains and vesicular aqueous cavities), a huge number of binding sites (RL
471 in the bioSUPRASs was in the range of 205-444 g·L⁻¹), different types of interactions
472 (ionic, polar, donor/acceptor hydrogen bonds and dispersion), and a broad vesicle size
473 range (from nm to μm). Combination of these properties enables the efficient extraction
474 of compounds in a wide polarity and size range through mixed-mode extraction
475 mechanisms.

476 Two highly water soluble synthetic dyes (trypan blue and malachite green) were extracted
477 from spiked tap water in order to prove the extraction capacity of bioSUPRASs. Trypan
478 blue is an anionic dye (**Figure ESI8 A**) with high molecular weight (868.85 g·mol⁻¹),
479 water solubility (up to 10 g·L⁻¹) and 4/20 donor/acceptor hydrogen bonds. Malachite
480 green is a cationic dye (**Figure ESI8 B**) with moderate molecular weight (329.46 g mol⁻¹)
481 ¹), high water solubility (up to 110 g·L⁻¹) and only one acceptor hydrogen bond.

482 **Table 2** shows the results for the extraction of the two dyes, expressed as percent
483 recovery. Three synthesis conditions were selected in order to study the effect of
484 bioSUPRAS composition on recoveries. Excellent results were obtained for malachite
485 green under all the conditions investigated, that suggesting that ionic attractive
486 interactions were an effective mechanism for the extraction of this highly water-soluble
487 dye. On the other hand, bioSUPRAS composition was determinant in the extraction of
488 trypan blue and the recovery increased from 53 to 94 % for bioSUPRAS 1 and 2,
489 respectively. As shown in **Table 2**, a higher concentration of RL was present in
490 bioSUPRAS 2 (31%, w/w) compared to bioSUPRAS 1 (19%, w/w), thus favouring the
491 partition of trypan blue. The dye was extracted by mixed mode mechanisms, so driving
492 extraction forces involved hydrogen bonding, dispersion and polar interactions at
493 bioSUPRAS phase and probably salting-out by NaCl too. The extraction with a higher
494 volume of bioSUPRAS (e.g. compare results for bioSUPRASs 2 and 3) did not improve
495 further the extraction of trypan blue.

496 These results illustrate how tailoring of bioSUPRAS composition provides a simple
497 strategy to improve extraction efficiencies of highly polar compounds.

498

499 **3.6 Compliance of bioSUPRASs with green solvent criteria**

500 The RL-based bioSUPRASs are fully or partially compliant with the twelve criteria set
501 for green solvents.⁷ Thus, regarding their *performance* they have shown potential to be
502 advantageous to conventional solvents employed in extraction processes in terms of
503 scope, efficiency and tailoring for different application strategies. As an example of this
504 potential we have discussed the efficient extraction of two highly water soluble
505 compounds from water, an application that would not be affordable with conventional
506 water immiscible organic solvents. Likewise, bioSUPRAS *synthesis* is carried out
507 through an energy-saving process (spontaneous coacervation at room temperature) that
508 has a high-atom economy (RL is virtually completely incorporated into the bioSUPRAS).

509 On the other hand, there are several criteria (*toxicity, biodegradability, stability and*
510 *flammability*) for which, bioSUPRAS characteristics should be closely related to their
511 components (RL and water). The low toxicity and high biodegradability under aerobic,
512 anoxic and anaerobic conditions of RLs have been widely confirmed.⁴⁷ Also, RLs are

513 thermally stable (boiling point around 170 °C) and non-flammable. So RL-based
514 SUPRASs are expected to be fully compliant with these criteria.

515 With respect to market criteria (*grade, price, availability and renewability*), we must
516 focus on RL since it is the main ingredient and determinant factor in the cost of
517 bioSUPRAS production. RLs are still in need of an economically available mass
518 production scheme,⁴⁴ and currently they are not economically competitive (\$20-25/kg)
519 compared to synthetic surfactants (e.g. \$1-3/kg).⁴³ The costs involved in RL production
520 originate from the raw materials to serve as carbon and nitrogen sources for the
521 microorganisms, the fermentation procedures and subsequent purification processes.⁴³
522 Many strategies have been developed to reduce the cost of each of these steps.^{43,44}
523 Specifically, RLs of different technical grade are available and the product purification
524 cost can be significantly lowered if cell-free fermentation broth or less purified RLs can
525 be used in place of purified RLs. Here, we have proved that bioSUPRASs are generated
526 from 90% purity RLs and future investigation should be conducted to study the formation
527 of bioSUPRASs from less purified RLs.

528 BioSUPRASs are formed in situ when they are applied to liquid samples, so the criterion
529 *storage* mainly applies to applications involving solid samples. Because of their
530 composition, bioSUPRASs fulfil all legislations to be safely transported and we verified
531 that they were stable in closed bottles for at least one month at room temperature.

532 Finally, regarding *recyclability*, we should consider the recovery of RL from the
533 bioSUPRASs and the salt from the synthesis equilibrium solution. In general, reported
534 purification/reuse strategies with non-volatile alternative solvents (deep eutectic solvents
535 and ionic liquids) are based on back-extraction of the target compounds with anti-solvents
536 for the extractant, evaporation/reconstitution steps and, in a lesser extent, solid-phase
537 extraction with macroporous resins (e.g. ME-2 polystyrene matrix, XAD-16 styrene-
538 divinylbenzene).⁶³ In this sense, RLs could be recovered from the final SUPRAS extracts
539 by precipitation in acidic medium (pK_a 5.6-5.9 for the carboxylic groups), by the addition
540 of a poor solvent (anionic RLs are poorly soluble in organic solvents as acetone or
541 acetonitrile), by increasing salt concentration (**Figure 1**) or by using ion exchange resins.
542 Regarding the leaching of SUPRAS components into treated liquid samples, since we
543 measured that ~100% of the surfactant was incorporated into the SUPRAS phase, only
544 traces of RLs would remain in the treated water and this should not be of concern due to
545 their eco-friendly properties. Nevertheless, since salty water is needed to promote

546 SUPRAS formation, when dealing with water samples, these processes would be
547 advantageous for treatment of seawater or salty industrial wastewater (e.g. textile and oil
548 mill wastewater). When solid samples would be treated, the bioSUPRAS would be first
549 generated and then separated from its equilibrium salty solution, before adding it to the
550 solid sample as it has been reported with SUPRAS made up of synthetic surfactants.⁶¹
551 The salty equilibrium solution could be used for the synthesis of new bioSUPRASs.
552 **Table ESI6** compares different SUPRAS that have reported for extraction processes⁶⁴⁻⁶⁹
553 in terms of environmental, health and sustainability concerns and the market price of the
554 surfactant.

555

556 **4. Conclusions**

557 To the best of our knowledge, bioSUPRASs produced from aqueous solutions of
558 rhamnolipids through salt-induced coacervation are described for the first time. These
559 biosolvents exhibit all the intrinsic properties of SUPRASs: versatile nanostructured
560 liquids, high efficient extractants and simple and quick procedures of synthesis, but they
561 are greener since synthetic surfactants, organic co-solvents, high concentration of acids
562 or high temperatures are not necessary for their production. That turns bioSUPRASs into
563 a green alternative to conventional solvents due to their biodegradability, low toxicity and
564 sustainability. This study revealed the first characterization of bioSUPRASs in terms of
565 composition, structure, and extraction capacity. It is expected that a greater knowledge
566 of these solvents helps to broaden their application in different fields, including the
567 treatment of wastewater with high saline concentration (e.g. brine in food industry),
568 sample treatment (extraction and clean-up) for analytical methods or the enrichment and
569 encapsulation of bioactive compounds.

570

571 **Acknowledgement**

572 Authors gratefully acknowledge financial support from Spanish Ministry of Science,
573 Innovation and Universities for the project CTQ2017-83823R, Ramón y Cajal contract
574 of A. Ballesteros-Gómez (RYC-2015-18482) and FPU grant (FPU15/03704) of E.
575 Romera-García. M. A. Martín Santos and I. Bellido Padillo from the Department of
576 Inorganic Chemistry and Chemical Engineering of the University of Córdoba are

577 acknowledged for the help in the measurement of sulfate in aqueous solutions. Authors
578 gratefully acknowledge the services provided by the Central Research Support Service
579 (SCAI) of the University of Córdoba and the Research, Technology and Innovation
580 Center of the University of Seville (CITIUS).

581 **References**

- 582 1. I. T. Horváth, *Green Chem.*, 2008, **10**, 1024–1028.
- 583 2. Global green solvents & bio solvents market forecast 2019-2027,
584 [https://www.inkwoodresearch.com/reports/global-green-solvents-bio-solvents-market-](https://www.inkwoodresearch.com/reports/global-green-solvents-bio-solvents-market-forecast-2019-2027/)
585 [forecast-2019-2027/](https://www.inkwoodresearch.com/reports/global-green-solvents-bio-solvents-market-forecast-2019-2027/), (accessed March 2020).
- 586 3. Regulation (EC) No 1907/2006 of the European Parliament and of the Council of 18
587 December 2006 concerning the Registration, Evaluation, Authorisation and Restriction
588 of Chemicals (REACH), establishing a European Chemicals Agency. Official Journal of
589 the European Union, L396, 30.12.2006, p1.
- 590 4. Frank R. Lautenberg Chemical Safety for the 21st Century Act. Public Law 114–182—
591 June 22, 2016, <https://www.congress.gov/114/plaws/publ182/PLAW-114publ182.pdf>,
592 (accessed March 2020).
- 593 5. W. M. Nelson, *Green solvents for chemistry: perspectives and practice*, Oxford
594 University Press, New York, 2003.
- 595 6. C. Capello, U. Fischer and K. Hungerbühler, *Green Chem.*, 2007, **9**, 927–934.
- 596 7. Y. Gu and F. Jérôme, *Chem. Soc. Rev.*, 2013, **42**, 9550-9570.
- 597 8. *The application of green solvents in separation processes*, ed. F. Pena-Pereira and M.
598 Tobiszewski, Elsevier, Amsterdam, 2017.
- 599 9. A. Zhu, L. Li, C. Zhang, Y. Shen, M. Tang, L. Bai, C. Du, S. Zhang and J. Wang,
600 *Green Chem.*, 2019, **21**, 307–313.
- 601 10. W. Chen, J. Jiang, X. Lan, X. Zhao, H. Mou and T. Mu, *Green Chem.*, 2019, **21**,
602 4748-4756.
- 603 11. A. Ballesteros-Gómez, M. D. Sicilia and S. Rubio, *Anal. Chim. Acta.*, 2010, **677**, 108-
604 130.
- 605 12. A. Ballesteros-Gómez, S. Rubio, and D. Pérez-Bendito, *J. Chromatogr. A*, 2009,
606 **1216**, 530–539.
- 607 13. J. A. Pelesko, *Self-assembly: The science of things that put themselves together*,
608 Chapman and Hall/CRC, Boca Ratón, 2007.
- 609 14. J. W. Steed, D. R. Turner and K. J. Wallace, *Core concepts in Supramolecular*
610 *Chemistry and Nanochemistry*, John Wiley & Sons, Chichester, 2007.

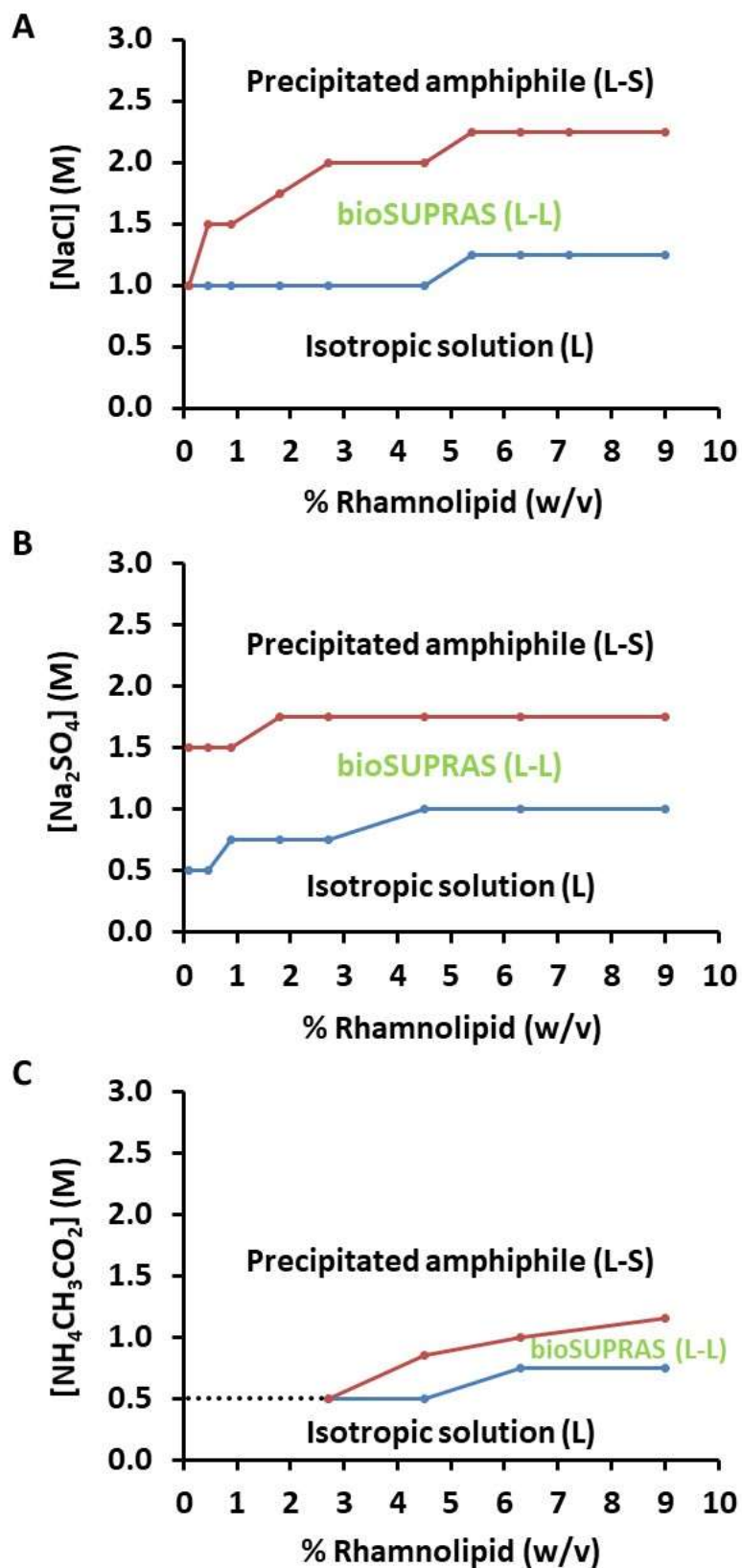
- 611 15. G. M. Whitesides and M. Boncheva, *Proc. Natl. Acad. Sci. U.S.A.*, 2002, **99**, 4769–
612 4774.
- 613 16. I. A. Sedova, M. A. Stolova and B. N. Solomonova, *J. Phys. Org. Chem.*, 2011, **24**
614 1088–1094.
- 615 17. D. F. Evans and H. Wennerström, *The Colloidal Domain: Where Physics, Chemistry,*
616 *Biology, and Technology Meet*, Wiley-VCH, New York, 1999.
- 617 18. D. Lombardo, M. A. Kiselev, S. Magazù and P. Calandra, *Adv. Cond. Matter Phys.*,
618 2015, 1-22.
- 619 19. H. G. Bungenberg de Jong and H. R. Kruyt, *Proc. Acad. Sci. Amsterdam*, 1929, **32**,
620 849-856.
- 621 20. D. H. Everett, *Pure Applied Chem.*, 1972, **31**, 577-638.
- 622 21. F. J. Ruiz, S. Rubio and D. Pérez-Bendito, *Anal. Chem.*, 2006, **78**, 7229–7239.
- 623 22. X. Jin, M. Zhu and E. D. Conte, *Anal. Chem.*, 1999, **71**, 514–517.
- 624 23. I. Casero, D. Sicilia, S. Rubio and D. Pérez-Bendito, *Anal. Chem.*, 1999, **71**, 4519–
625 4526.
- 626 24. B. Yao and L. Yang, *J. Colloid Interface Sci.*, 2008, **319**, 316–321.
- 627 25. A. Ballesteros-Gómez and S. Rubio, *Anal. Chem.*, 2012, **84**, 342-349.
- 628 26. F. J. Ruiz, S. Rubio and D. Pérez-Bendito, *Anal. Chem.*, 2007, **79**, 7473–7484.
- 629 27. J. A. Salatti-Dorado, S. González-Rubio, D. García-Gómez, R. Lucena, S. Cárdenas
630 and S. Rubio, *Anal. Chim. Acta*, 2019, **1046**, 132-139.
- 631 28. A. Melnyk, J. Namieśnik and L. Wolska, *Trends Anal. Chem.*, 2015, **71**, 282–292.
- 632 29. S. Rubio, *Anal. Bioanal. Chem.*, 2020, DOI: 10.1007/s00216-020-02559-y.
- 633 30. J. R. Bacon, O. T. Butler, W. R. L. Cairns, J. M. Cook, R. Mertz-Krause and J. F.
634 Tyson, *J. Anal. At. Spectrom.*, 2019, **34**, 9-58.
- 635 31. J. P. McCord, D. C. Muddiman and M. G. Khaledi, *J. Chromatogr. A*, 2017, **1523**,
636 293–299.
- 637 32. J. A. Asenjo and B. A. Andrews, *J. Chromatogr. A*, 2011, **1218**, 8826-8835.

- 638 33. M. D. S. Noorashikin, N. M. Sohaimi, N. Suda, H. Z. Aziz, S. R. M. Zaini, S.
639 Kandasamy and K. Suresh, *J. Sust. Sci. Manag.*, 2017, **12**, 79-95.
- 640 34. L. S. Torres-Valenzuela, A. Ballesteros-Gómez and S. Rubio, *Environ. Sci.: Water*
641 *Res. Technol.*, 2020, **6**, 757-766.
- 642 35. L. S. Torres-Valenzuela, A. Ballesteros-Gómez, A. Sanin and S. Rubio, *Sep. Pur.*
643 *Technol.*, 2019, **228**, 115759.
- 644 36. A. Ballesteros-Gómez, N. Caballero-Casero, S. García-Fonseca, L. Lunar, and S.
645 Rubio, *Chemosphere*, 2019, **223**, 569-576.
- 646 37. R. P. F. Melo, E. L. Barros Neto, M. C. P. A. Moura, T. N. Castro Dantas, A. A.
647 Dantas Neto and H. N. M. Oliveira, *Separ. Purif. Technol.*, 2014, **138**, 71-76.
- 648 38. J. A. Salatti-Dorado, D. García-Gómez, V. Rodríguez-Ruiz, V. Gueguen, G. Pavon-
649 Djavid and S. Rubio, *Food Chem.*, 2019, **279**, 294–302.
- 650 39. L. S. Torres-Valenzuela, A. Ballesteros-Gómez and S. Rubio, *J. Food. Eng.*, 2020,
651 **278**, 109933.
- 652 40. M. N. Keddar, A. Ballesteros-Gómez, M. Amiali, J.A. Siles, D. Zerrouki, M. A.
653 Martín and S. Rubio, *Sep. Purif. Technol.*, 2020, **251**, 117327.
- 654 41. D. K. F. Santos, R. D. Rufino, J. M. Luna, V. A. Santos and L. A. Sarubbo, *Int. J.*
655 *Mol. Sci.*, 2016, **17**, 401-432.
- 656 42. C. F. C. Rosa, D. M. G. Freire and H. C. Ferraz, *J. Environ. Chem. Eng.*, 2015, **3**, 89–
657 94.
- 658 43. H. Chong and Q. Li, *Microb. Cell. Fact.*, 2017, **16**,137.
- 659 44. J. Jiang, Y. Zu, X. Li, Q. Meng and X. Long, *Bioresour. Technol.*, 2020, **298**, 122394.
- 660 45. T. Tiso, in *Consequences of Microbial Interactions with Hydrocarbons, Oils, and*
661 *Lipids: Production of Fuels and Chemicals. Handbook of Hydrocarbon and Lipid*
662 *Microbiology*, ed. S. Y. Lee, Springer, Cham, 2018, *Rhamnolipids: Production,*
663 *Performance, and Application*, 587-622.
- 664 46. K. K. S. Randhawa and P. K. S. M. Rahman, *Front. Microbiol.*, 2014, **5**, 454.
- 665 47. G. Liu, H. Zhong, X. Yang, Y. Liu, B. Shao and Z. Liu, *Biotechnol. Bioeng.*, 2017,
666 1–19.

- 667 48. A. I. Rodrigues, E. J. Gudiña, J. A. Teixeira and L. R. Rodrigues, *Sci. Rep.*, 2017, **7**,
668 12907.
- 669 49. M. L. Chen, J. Penfold, R. K. Thomas, T. J. P. Smyth, A. Perfumo, R. Marchant, I.
670 M. Banat, P. Stevenson, A. Parry, I. Tucker and I. Grillo, *Langmuir*, 2010, **26**, 18281–
671 18292.
- 672 50. I. E. Kłosowska-Chomiczewska, K. Mędrzycka, E. Hallmann, E. Karpenko, T.
673 Pokynbroda, A. Macierzanka and C. Jungnickel, *J. Colloid Interf. Sci.*, 2017, **488**, 10-19.
- 674 51. T. Imura, H. Yanagishita, and D. Kitamoto, *J. Am. Chem. Soc.*, 2004, **126**, 10804-
675 10805.
- 676 52. M. Sánchez, F. J. Aranda, M. J. Espuny, A. Marqués, J. A. Teruel, A. Manresa and
677 A. Ortiz, *J. Colloid Interf. Sci.*, 2007, **307**, 246–253
- 678 53. H. Abbasi, K. A. Noghabi, M. M. Hamed, H. S. Zahiri, A. A. Moosavi-Movahedi,
679 M. Amanlou, J. A. Teruel and A. Ortiz, *Colloids Surf. B Biointerfaces*, 2013, **101**, 256–
680 265
- 681 54. Ş. Ş. Helvacı, S. Peker and G. Özdemir, *Colloids Surf. B Biointerfaces*, 2004, **35**,
682 225–233.
- 683 55. J. Appell and G. Porte, *J. Phys. Lett.*, 1983, **44**, 689-695.
- 684 56. S. Kumar, D. Sharma, Z. A. Khan and K. Din, *Langmuir*, 2002, **18**, 4205-4209.
- 685 57. N. Vlachy, M. Drechsler, J. M. Verbavatz, D. Touraud and W. Kunz, *J. Colloid*
686 *Interface Sci.*, 2008, **319**, 542-548.
- 687 58. W. Kunz, *Curr. Opin. Colloid Interface Sci.*, 2010, **15**, 34–39.
- 688 59. A. Salis and B. W. Ninham, *Chem. Soc. Rev.*, 2014, **43**, 7358-7377.
- 689 60. I. D. Kuntz, *J. Am. Chem. Soc.*, 1971, **93**, 514–516.
- 690 61. C. Caballo, M. D. Sicilia and S. Rubio, in *The application of green solvents in*
691 *separation processes*, ed. F. Pena-Pereira and M. Tobiszewski, Elsevier, Amsterdam,
692 2017, **5**, 111-137.
- 693 62. Y. P. Guo, Y. Y. Hu, R. R. Gub, and H. Lin, *J. Colloid Interf. Sci.*, 2009, **331**, 356-
694 363.

- 695 63. L S. Torres-Valenzuela, A. Ballesteros-Gómez and S. Rubio, *Food Eng. Rev.*, 2020,
696 **12**, 83–100.
- 697 64. V. Cardeñosa, M. L. Lunar and S. Rubio, *J. Chromatogr. A*, 2011, **1218**, 8996-9002.
- 698 65. L. Chen, Q. Zhao, H. Jin, X. Zhang, Y. Xu, A. Yu, H. Zhang and L. Ding, *Talanta*,
699 2010, **18**, 692-697.
- 700 66. I. Casero, D. Sicilia, S. Rubio and D. Pérez-Bendito, *Anal. Chem.* 1999, **71**, 4519–
701 4526.
- 702 67. A. P. Nambiar, M. Sanyal and P. S. Shrivastav, *Food Anal. Methods*, 2017, **10**, 3471–
703 3480.
- 704 68. N. Luque, A. Ballesteros-Gómez, S. van Leeuwen and S. Rubio, *J. Chromatogr. A*,
705 2012, **1235**, 84-91.
- 706 69. X. Jin., M. Zhou and E. D. Conte, *Anal. Chem.*, 1999, **71**, 514–517.

707 **Figure 1.** Phase diagrams of ternary mixtures of rhamnolipid/water/salt (A: NaCl; B:
 708 Na₂SO₄; C: NH₄CH₃CO₂) at 25 °C. Concentration of salt (M) is plotted versus
 709 concentration of rhamnolipid (% w/v) in the synthesis mixture



710

Figure 2. Volume of bioSUPRAS ($\mu\text{L}\cdot\text{mL}^{-1}$ mixture) as a function of the initial concentration of rhamnolipid (% w/v) (A: NaCl; B: Na_2SO_4) and salt (M) (C: NaCl; D: Na_2SO_4)

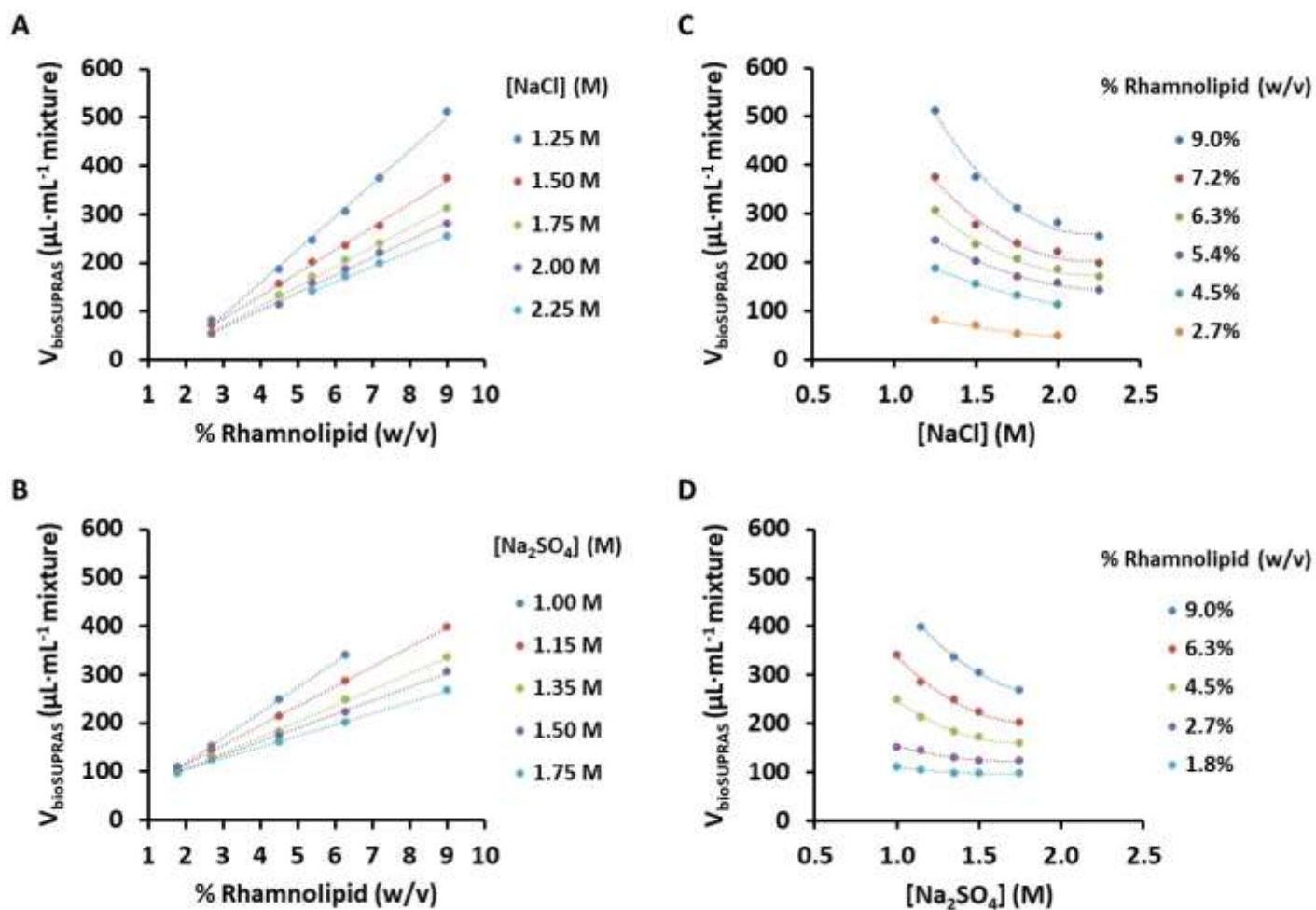


Figure 3. Intensity-based aggregate size distribution of bioSUPRASs synthesized from mixtures containing 4.5% of rhamnolipid (w/v) and different concentrations of NaCl (A: 1.25 M; B; 1.50 M; C: 1.75 M). Measurements were carried out by DLS at 173° scattering angle and 25 °C

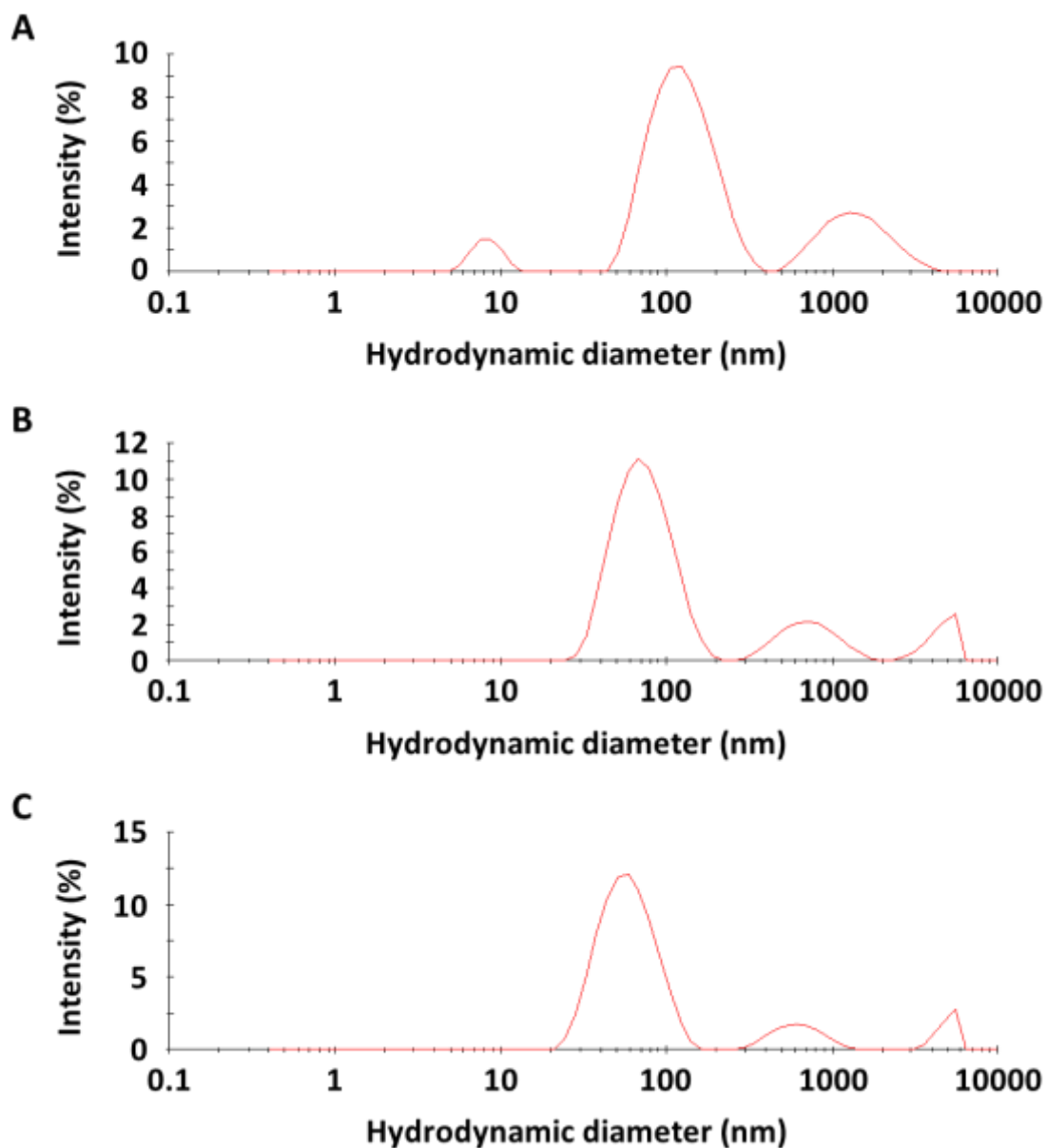
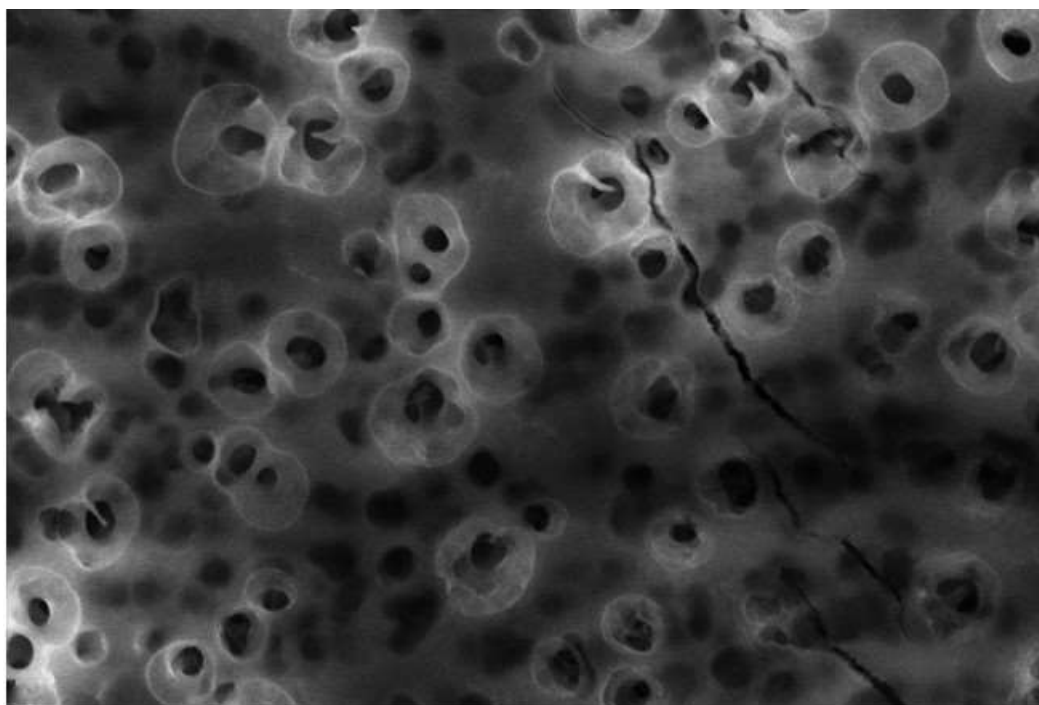
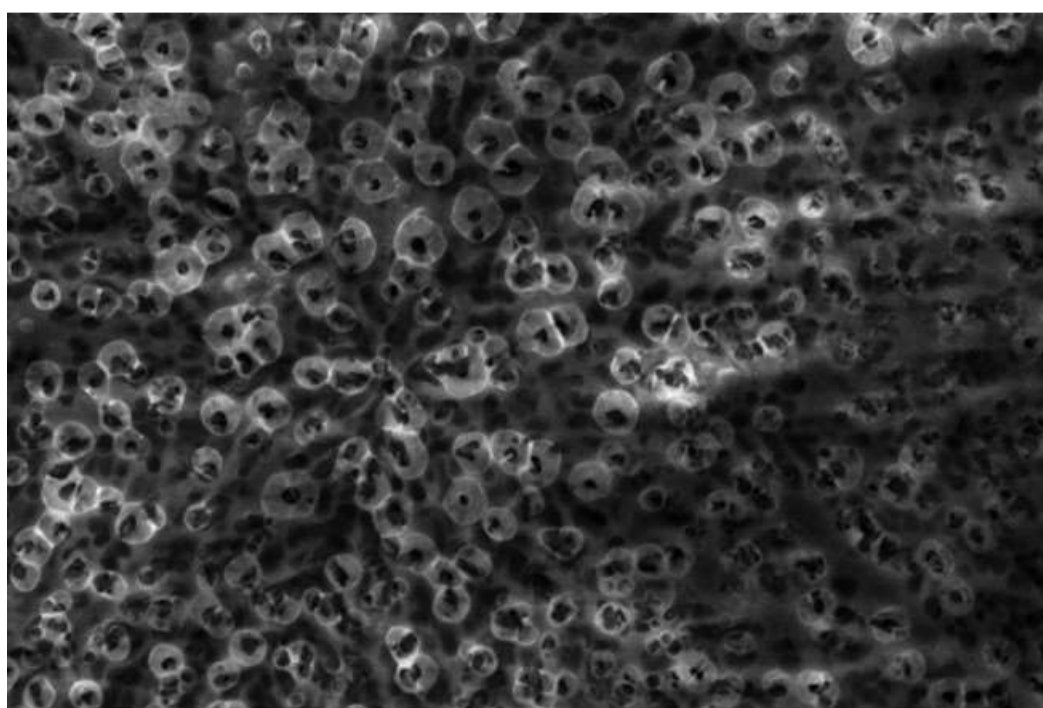


Figure 4. Cryo-SEM micrographs of a bioSUPRAS synthesized from a mixture containing 4.5% of rhamnolipid (w/v) and 1.5 M of Na_2SO_4

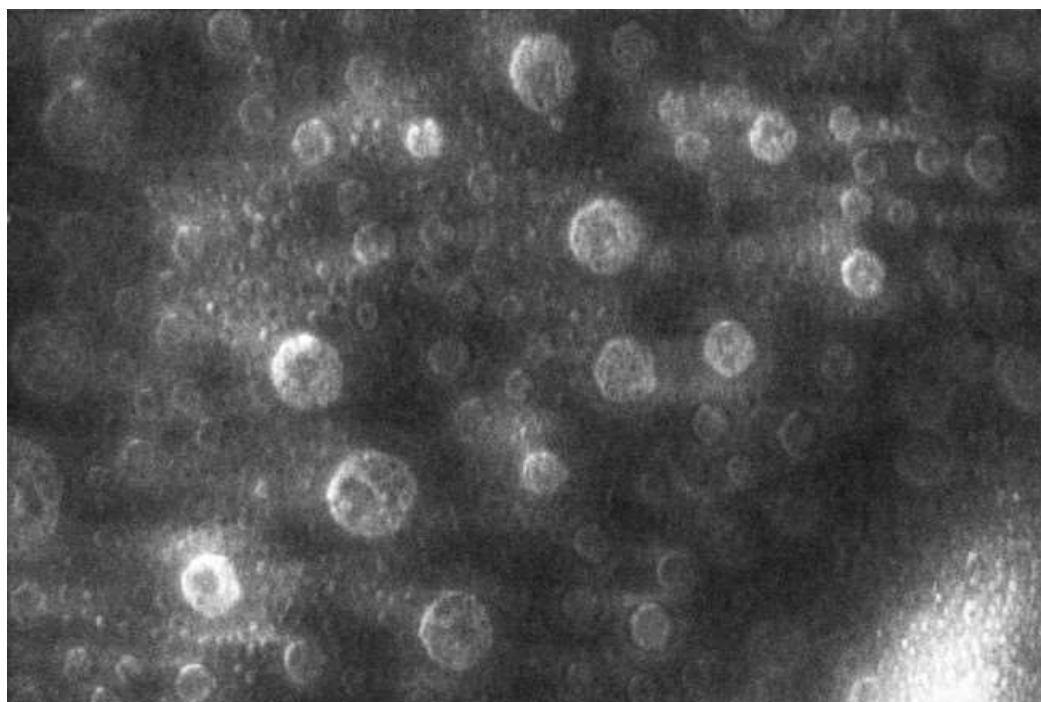


—| 1 μm

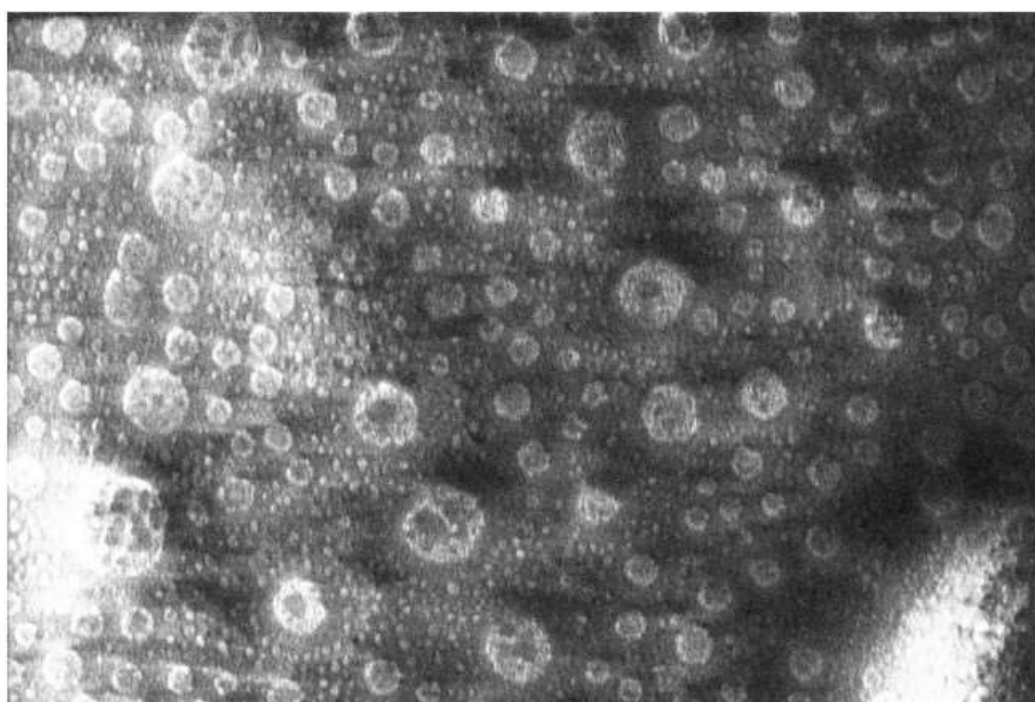


—| 2 μm

Figure 5. Cryo-SEM micrographs of a bioSUPRAS synthesized from a mixture containing 4.5% of rhamnolipid (w/v) and 1.5 M of NaCl



2 μm



10 μm

Table 1. Composition of bioSUPRASs formed from different coacervation conditions

<i>Synthesis conditions</i>		<i>bioSUPRAS composition</i>	
¹ [NaCl] (M)	% H ₂ O±SD (w/w)	% Rhamnolipid±SD (w/w)	% Salt±SD (w/w)
1.00	77±2	19±3	4.5±0.3
1.25	73±5	24±5	5.3±0.2
1.50	68±4	31±4	6.0±0.1
1.75	64±5	33±4	6.5±0.1
2.00	60±3	37±3	7.0±0.4
2.25	55±3	40±2	7.2±0.6
¹ [Na ₂ SO ₄] (M)	% H ₂ O±SD (w/w)	% Rhamnolipid±SD (w/w)	% Salt±SD (w/w)
1.00	71±7	19±2	10.1±0.4
1.15	65±3	26±1	10.7±0.7
1.35	60±4	29±1	11.4±0.7
1.50	56±5	36±3	12±1
1.75	50±6	40±2	12±1
² % Rhamnolipid±SD (w/v)	% H ₂ O±SD (w/w)	% Rhamnolipid±SD (w/w)	% Salt±SD (w/w)
2.7	58±4	38±1	6.8±0.4
4.5	59.9±0.8	37±3	7.0±0.2
5.4	60±4	38±2	7.0±0.3
6.3	60.7±0.4	38±4	7.1±0.1
9.0	60.9±0.9	37±1	7.1±0.7
³ % Rhamnolipid±SD (w/v)	% H ₂ O±SD (w/w)	% Rhamnolipid±SD (w/w)	% Salt±SD (w/w)
1.8	59±4	30±3	11.3±0.7
2.7	60±4	28±2	11.4±0.7
4.5	59±3	28±2	11.3±0.3
6.3	60±3	29±3	11±1
9.0	59±2	29±2	11±1

¹Percentages of H₂O and rhamnolipid in the bioSUPRAS are mean values for RL concentrations in the interval of 1.8-9 % (w/v); ²NaCl: 2 M; ³Na₂SO₄: 1.35 M.

Table 2. Mean percent recoveries obtained for the extraction of trypan blue and malachite green in spiked tap water with different bioSUPRASs

	<i>Synthesis conditions</i>		<i>bioSUPRAS</i>	<i>Recovery±SD (%)</i>	
	% Rhamnolipid (w/v)	[NaCl] (M)	% Rhamnolipid (w/w)	Trypan blue	Malachite green
1	0.9	1	19	53±3	100.3±0.3
2	0.9	1.5	31	94.2±0.1	100.1±0.4
3	4.5	1.5	31	90.8±0.5	92±2